Proton-Coupled Electron Transfer of Cytochrome *c*

Daniel H. Murgida and Peter Hildebrandt*

Contribution from the Max-Planck-Institut für Strahlenchemie, Stiftstrasse 34-36, D-45470 Mülheim, Germany

Received December 4, 2000

Abstract: Cytochrome *c* (Cyt-*c*) was electrostatically bound to self-assembled monolayers (SAM) on an Ag electrode, which are formed by *ω*-carboxyl alkanethiols of different chain lengths (C_x). The dynamics of the electron-transfer (ET) reaction of the adsorbed heme protein, initiated by a rapid potential jump to the redox potential, was monitored by time-resolved surface enhanced resonance Raman (SERR) spectroscopy. Under conditions of the present experiments, only the reduced and oxidized forms of the native protein state contribute to the SERR spectra. Thus, the data obtained from the spectra were described by a one-step relaxation process yielding the rate constants of the ET between the adsorbed Cyt-*c* and the electrode for a driving force of zero electronvolts. For C_{16}- and C_{11}-SAMs, the respective rate constants of 0.073 and 43 s^{-1} correspond to an exponential distance dependence of the ET ($\beta = 1.28$ Å^{-1}), very similar to that observed for long-range intramolecular ET of redox proteins. Upon further decreasing the chain length, the rate constant only slightly increases to 134 s^{-1} at C_6- and remains essentially unchanged at C_3- and C_2-SAMs. The onset of the nonexponential distance dependence is paralleled by a kinetic H/D effect that increases from 1.2 at C_6- to 4.0 at C_2-coatings, indicating a coupling of the redox reaction with proton-transfer (PT) steps. These PT processes are attributed to the rearrangement of the hydrogen-bonding network of the protein associated with the transition between the oxidized and reduced state of Cyt-*c*. Since this unusual kinetic behavior has not been observed for electron-transferring proteins in solution, it is concluded that at the Ag/SAM interface the energy barrier for the PT processes of the adsorbed Cyt-*c* is raised by the electric field. This effect increases upon reducing the distance to the electrode, until nuclear tunneling becomes the rate-limiting step of the redox process. The electric field dependence of the proton-coupled ET may represent a possible mechanism for controlling biological redox reactions via changes of the transmembrane potential.

Introduction

The soluble monoheme protein cytochrome *c* (Cyt-*c*) acts as an electron carrier in the respiratory chain of aerobic organism.[1] It transfers electrons between the enzyme complexes cytochrome *c* reductase and cytochrome *c* oxidase which are both embedded in the mitochondrial membrane. The crucial role of Cyt-*c* in the redox chain of mitochondria has inspired a large number of experimental studies dedicated to elucidate the mechanism of interprotein electron-transfer (ET) processes.[2] Furthermore, Cyt-*c* has also attracted the interest of many research groups in a wider sense. Due to the early availability of well-resolved three-dimensional structures and site-specifically mutated protein variants,[3] Cyt-*c* has become *the* model system for studying long-range intra- and intermolecular ET of proteins.[4]

One of the most important experimental approaches is based on the covalent attachment of additional photoactive redox labels at different position of the protein surface of Cyt-*c* variants.[4a] Upon photoexcitation, ET reactions between these redox labels, in general Ru(II) complexes, and the heme are initiated. In this way, ET rate constant were determined for different ET distances and pathways. These experimental data have been interpreted in terms of different theoretical models which neglect or emphasize to different extents the dedicated ET pathways through the protein.[5]

In recent years, electrochemical devices have opened new possibilities for studying the redox process of Cyt-*c* and related heme proteins.[6] Biocompatible electrode coatings, that are based on self-assembled monolayers of alkanethiol derivatives (Figure 1),[7] guarantee a (quasi-)reversible voltammetric response, so

* Corresponding author. E-mail: hildebrandt@mpi-muelheim.mpg.de. Fax: +49 208 306 3951.

(1) (a) *Cytochrome c - Biological Aspects*; Pettigrew, G. W., Moore, G. R., Eds.; Springer-Verlag: Berlin, 1987. (b) *Cytochrome c. A Multidisciplinary Approach*; Scott, R. A., Mauk, A. G., Eds.; University Science Books: Sausalito, CA, 1995.

(2) (a) Millet, F. In *Cytochrome c. A Multidisciplinary Approach*; Scott, R. A., Mauk, A. G., Eds.; University Science Books: Sausalito, CA, 1995; Chapter 13 and references therein. (b) Gren, L. M.; Beasley, J. R.; Fine, B. R.; Saunders, A. J.; Hibdon, S.; Pielak, G. J.; Durham, B.; Millet, F. *J. Biol. Chem.* **1995**, *270*, 2466. (c) Wang, K.; Zhen, Y.; Sadoski, R.; Grinelli, S.; Gren, L.; Ferguson-Miller, S.; Durham, B.; Millet, F. *J. Biol. Chem.* **1999**, *274*, 38042.

(3) (a) Brayer, G. D.; Murphy, M. E. P. In *Cytochrome c. A Multidisciplinary Approach*; Scott, R. A., Mauk, A. G., Eds.; University Science Books: Sausalito, CA, 1995; Chapter 3 and references therein. (b) Berghuis, A. M.; Brayer, G. D. *J. Mol. Biol.* **1992**, *223*, 959.

(4) (a) Scott, R. A. In *Cytochrome c. A Multidisciplinary Approach*; Scott, R. A., Mauk, A. G., Eds.; University Science Books: Sausalito, CA, 1995; Chapter 15 and references therein. (b) Wishart, J. F.; Sun, J.; Cho, M.; Su, C.; Isied, S. S. *J. Phys. Chem. B* **1997**, *101*, 687.

(5) (a) Beratan, D. N.; Betts, J. N.; Onuchic, J. N. *Science* **1991**, *252*, 1285. (b) Moser, C. C.; Keske, J. M.; Warnicke, K.; Farid, R.; Dutton, P. L. *Nature* **1992**, *355*, 796. (c) Langen, R.; Coton, J. L.; Casimoro, D. R.; Karpishin, T. B.; Winkler, J. R.; Gray, H. B. *J. Biol. Inorg. Chem.* **1996**, *1*, 221. (d) Skourtis, S. S.; Beratan, D. N. *J. Biol. Inorg. Chem.* **1997**, *2*, 378. (e) Williams, R. J. P. *J. Solid State Chem.* **1999**, *145*, 488. (f) Winkler, J. R. *Curr. Opin. Chem. Biol.* **2000**, *4*, 192.

(6) (a) Bond, A. M.; Hill, H. A. O. In *Metal Ions in Biological Systems*; Sigel, H., Sigel, A., Eds.; Marcel Dekker: New York, 1991; Vol. 27, p 431. (b) Armstrong, F. A.; Wilson, G. S. *Electrochim. Acta* **2000**, *45*, 2623.

(7) Ulman, A. *Introduction to Ultrathin Organic Films. From Langmuir−Blodgett to Self-Assembly*; Academic Press: Boston, 1991; p 279 and references therein.

10.1021/ja004165j CCC: $20.00
Published on Web 04/04/2001

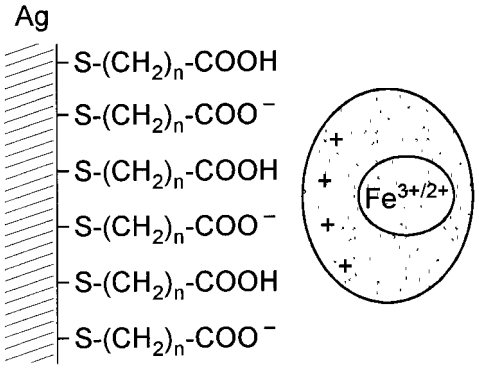

Figure 1. Schematic representation of Cyt-*c* electrostatically adsorbed to the SAM-coated Ag electrode.

that the determination of ET kinetics is also possible.[8,9] Such approaches represent a reliable alternative for determining not only the distance dependence but also the reorganization energy of the ET process. Furthermore, coatings may be designed to mimic charged interaction domains of the respective partner proteins so that the analysis of ET reaction at such devices may provide information about parameters specifically controlling *inter*molecular ET. In fact, previous electrochemical studies have indicated that thermodynamic and kinetic properties of the redox process are different when Cyt-*c* is electrostatically adsorbed to the SAM-coated electrode as compared to Cyt-*c* only weakly interacting with the monolayer.[8,9] Specifically, adsorbed Cyt-*c* was found to exhibit a shift of the redox potential, a lowering of the reorganization energy, and a nonexponential distance dependence of the observed ET rate constant.[8] However, the molecular processes that are responsible for these differences of the redox properties cannot be elucidated solely based on electrochemical techniques.

Stationary and time-resolved surface-enhanced resonance Raman (SERR) spectroscopy represents a powerful alternative approach, inasmuch as this technique allows the determination of the interfacial potential-dependent equilibria and reactions by probing the vibrational spectra of the heme groups of the adsorbed Cyt-*c* exclusively.[10−12] SERR spectroscopy has successfully been employed for heme proteins adsorbed on bare Ag electrodes,[10−14] and was recently extended to Ag electrodes coated with SAMs.[15−17] In this way, it was shown that the electric field at the Ag/SAM/electrolyte interface controls the orientation of the adsorbed protein and may cause structural changes in the heme pocket of Cyt-*c* which in turn have a pronounced effect on the redox potential.[16,17] Thus, the mechanism and dynamics of the interfacial redox reaction may display a rather complex behavior. Consequently, rate constants determined by electrochemical techniques do not necessarily correspond to "pure" ET rate constants but may reflect coupled or gated processes similar to complex enzymatic reaction sequences.[18]

The time-resolved SERR experiments presented in this study are dedicated to disentangle the interfacial redox process of Cyt-*c* and to analyze the kinetics of the heterogeneous ET between the adsorbed Cyt-*c* and the SAM-coated Ag electrode using monolayers of different chain lengths. Specifically, we were interested to determine the electric field dependence of the interfacial ET.

Materials and Methods

Chemicals. Mercaptoacetic acid (C_2), 3-mercaptopropionic acid (C_3), 11-mercaptoundecanoic acid (C_{11}), and 16-mercaptohexadecanoic acid (C_{16}) were purchased from Sigma and used without further purification. 6-Mercaptohexanoic acid (C_6) was synthesized according to published procedures,[19] and purified by HPLC. Horse heart cytochrome *c* (Cyt-*c*; Sigma) was purified as previously published.[11]

SERR Spectroscopy. SERR spectra were measured with 413-nm cw-excitation using a Kr-ion laser (Coherent 302) with a power of ~50 mW at the sample. The scattered light (90°) was focused onto the entrance slit of a double monochromator (ISA, U1000) working as a spectrograph and equipped with a liquid-nitrogen-cooled CCD camera. The spectral bandwidth was 4 cm^{-1}, and the increment per data point was 0.53 cm^{-1}. The total accumulation time of the stationary and time-resolved SERR spectra was ~10 and 5 s, respectively. SERR experiments were carried out with a rotating electrode to avoid degradation processes caused by laser-induced heating. A detailed description of the home-built electrode and the electrochemical cell is given elsewhere.[16] All potentials cited in this work refer to the saturated calomel electrode (SCE).

The preparation of the SER-active SAM-coated Ag electrodes was described elsewhere.[16] Modified electrodes were placed into the electrochemical cell containing 0.2 μM Cyt-*c* and 12.5 mM potassium phosphate buffer and 12.5 mM K_2SO_4 as supporting electrolyte, either in H_2O or D_2O at pH 7.0. The electrode was kept at open circuit for 45 min to establish adsorption equilibrium. Under these conditions, the adsorbed Cyt-*c* is exclusively in the native conformational state denoted as B1.[16] Conversely, the Cyt-*c* concentration in the bulk was sufficiently low to avoid any interference of the SERR spectra by resonance Raman signals from the dissolved protein.[16] All of the experiments were repeated several times to ensure reproducibility. After background subtraction the SERR spectra were subjected to a component analysis in which complete spectra of the individual species are fitted to the measured spectra.[12,14b,c,16,17,20]

Time-Resolved SERR Experiments. Time-resolved SERR experiments were carried out by applying a rapid potential jump and probing of the relaxation process during a measuring interval Δt by SERR spectroscopy. The underlying principles of this approach have been described elsewhere.[12] In the present work, the previous setup was modified in two aspects. First, the mechanical chopper that was used for gating the exciting laser beam was replaced by an electronically

(8) (a) Tarlov, M. J.; Bowden, E. F. *J. Am. Chem. Soc.* **1991**, *113*, 1847. (b) Cooper, J. M.; Greenough, K. R.; McNeil, C. J. *J. Electroanal. Chem.* **1993**, *347*, 297. (c) Song, S.; Clark, R. A.; Bowden, E. F.; Tarlov, M. J. *J. Phys. Chem.* **1993**, *97*, 6564. (d) Feng, Z. Q.; Imabayashi, S.; Kakiuchi, T.; Niki, K. *J. Electroanal. Chem.* **1995**, *394*, 149. (e) Nahir, T. M.; Bowden, E. F. *J. Electroanal. Chem.* **1996**, *410*, 9. (f) Clark, R. A.; Bowden, E. F. *Langmuir* **1997**, *113*, 559. (g) Feng, Z. Q.; Imabayashi, S.; Kakiuchi, T.; Niki, K. *J. Chem. Soc., Faraday Trans.* **1997**, *93*, 1367. (h) El Kasmi, A.; Wallace, J. M.; Bowden, E. F.; Binet, S. M.; Linderman, R. J. *J. Am. Chem. Soc.* **1998**, *120*, 225. (i) Ruzgas, T.; Wong, L.; Gaigalas, A. K.; Vilker, V. L. *J. Electroanal. Chem.* **1999**, *465*, 96. (j) Gaigalas, A. K.; Ruzgas, T. *J. Electroanal. Chem.* **1999**, *465*, 96. (k) Avila, A.; Gregory, B. W.; Niki, K.; Cotton, T. M. *J. Phys. Chem. B* **2000**, *104*, 2759.

(9) (a) Terrettaz, S.; Cheng, J.; Miller, C. J. *J. Am. Chem. Soc.* **1996**, *118*, 7857. (b) Cheng, J.; Terrettaz, S.; Blankman, J. I.; Miller, C. J.; Dangi, B.; Guiles, R. D. *Isr. J. Chem.* **1997**, *37*, 259.

(10) Cotton, T. M.; Schultz, S. G.; Van Duyne, R. P. *J. Am. Chem. Soc.* **1980**, *102*, 7962.

(11) Hildebrandt, P.; Stockburger, M. *Biochemistry* **1989**, *28*, 6710.

(12) Wackerbarth, H.; Klar, U.; Günther, W.; Hildebrandt, P. *Appl. Spectrosc.* **1999**, *53*, 283.

(13) Cotton, T. M.; Timkovich, R.; Cork, M. S. *FEBS Lett.* **1981**, *133*, 39.

(14) (a) Lecomte, S.; Wackerbarth, H.; Hildebrandt, P.; Soulimane, T.; Buse, G. *J. Raman Spectrosc.* **1998**, *29*, 687. (b) Lecomte, S.; Wackerbarth, H.; Soulimane, T.; Buse, G.; Hildebrandt, P. *J. Am. Chem. Soc.* **1998**, *120*, 7381. (c) Lecomte, S.; Hildebrandt, P.; Soulimane, T. *J. Phys. Chem. B* **1999**, *103*, 10053.

(15) (a) Maeda, Y.; Yamamoto, H.; Kitano, H. *J. Phys. Chem.* **1995**, 99, 4837. (b) Hobara, D.; Niki, K.; Cotton, T. M. *Biospectroscopy* **1998**, *4*, 161.

(16) Murgida, D. H.; Hildebrandt, P. *J. Phys. Chem. B*, **2001**, *105*, 1578.

(17) (a) Murgida, D. H.; Hildebrandt, P. *J. Mol. Struct.* **2000**, in press. (b) Murgida, D. H.; Hildebrandt, P. *Angew. Chem. Int. Ed.* **2001**, *40*, 728.

(18) Davidson, V. L. *Acc. Chem. Res.* **2000**, *33*, 87.

(19) Bain, C. D.; Troughton, E. B.; Tao, Y. T.; Evall, E.; Whitesides, G. M.; Nuzzo, R. G. *J. Am. Chem. Soc.* **1989**, *111*, 321.

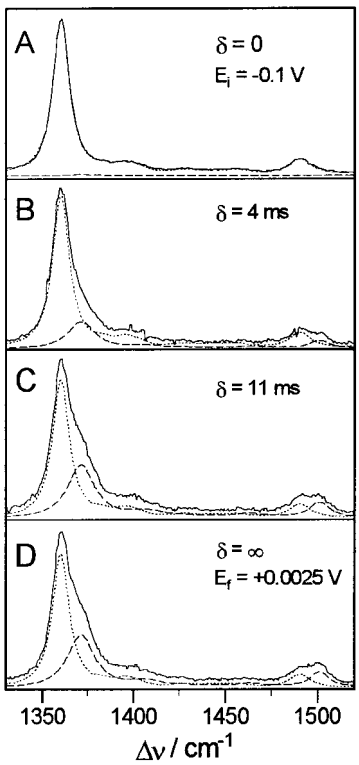

Figure 2. Stationary and time-resolved SERR spectra of Cyt-*c* adsorbed on a C_2-coated Ag electrode measured with 413-nm excitation. (A) stationary SERR spectrum measured at the initial potential of $E_i = -0.1$ V; (B, C) time-resolved SERR spectra measured at different delay times δ after the potential jump from $E_i = -0.1$ V to $E_f = +0.0025$ V; (D) stationary SERR spectrum measured at the final potential of $E_f = +0.0025$ V. The component spectra of the reduced and oxidized forms of Cyt-*c* are represented by the dotted and dashed lines, respectively.

controlled intensity modulator equipped with a pulse amplifier (LM 0202, LIV8, Gsänger, Planegg) which allows a precise adjustment of Δt down to the nanosecond time scale. Second, synchronization and timing of the potential jumps, delay times δ, and measuring intervals are now achieved by a home-built multichannel pulse delay generator. This modified device provides a high accuracy of time-controlling of the individual events in a wide dynamic range that spans from 1 μs to 100 s. Thus, the time-resolution of this approach is exclusively limited by the response time of the electrochemical cell which was determined to be <150 μs.

Results

SERR Spectroscopy of the Adsorbed Cytochrome *c*. SERR spectra were measured in the region between 1300 and 1650 cm^{-1} which has been shown to allow a reliable quantitative spectra analysis.[11,12,14,16,17] The bands in this spectral range are characteristic of the oxidation, spin, and ligation state of the heme iron[21] and, hence, are appropriate for distinguishing between different states of Cyt-*c*. As an example, Figure 2 shows stationary and time-resolved SERR spectra of Cyt-*c* adsorbed on C_2-coated electrodes. At a potential of -100 mV, the stationary SERR spectrum exclusively displays marker bands of the reduced (native) state B1, which, in the region displayed in that figure, are the bands ν_4 and ν_3 at 1360 and 1491 cm^{-1}, respectively (Figure 2A). In the SERR spectrum measured at the redox potential of Cyt-*c* on C_2-coated electrodes (2.5 mV),[16] the ν_4 and ν_3 bands of the oxidized form of B1 are clearly detectable at 1371 and 1501 cm^{-1}, respectively (Figure 2D). Since the component spectra of both species are known, the quantitative analysis of the measured SERR spectra is straightforward and unambiguous inasmuch as the only variables in the fitting routine are the amplitudes of the component spectra involved. The spectral contributions of the individual species obtained in this way are then converted into relative concentrations on the basis of the relative scattering cross sections determined previously.[22] The same procedure was applied to the spectral analysis of the time-resolved spectra.

Time-Resolved SERR Spectroscopy. Figure 2B,C shows two of the time-resolved SERR spectra of Cyt-*c* on C_2-coated electrodes measured for the potential jump from -100 mV to the redox potential of 2.5 mV at variable delay times. It can clearly be seen that already at $\delta = 4$ ms there is a substantial increase of the oxidized species which has almost reached its equilibrium value at $\delta = 11$ ms. No spectral contributions from different Cyt-*c* species other than the native state B1 could be detected in the stationary and time-resolved SERR spectra. Thus, the kinetic analysis of the data derived from the time-resolved SERR spectra can follow a simple one-step relaxation process, that is the ET of the native state B1 of the adsorbed Cyt-*c*. Then one obtains

$$\frac{\Delta[B1_{red}]_{\delta'}}{\Delta[B1_{red}]_0} = \exp\left(-\frac{t}{\tau}\right) \quad (1)$$

with $\Delta[B1_{red}]_{\delta'}$ and $\Delta[B1_{red}]_0$ denoting concentration differences of the reduced form of B1 ($B1_{red}$) with respect to the equilibrium values at the final potential E_f for $\delta' = \delta + \Delta t/2$ and $t = 0$, respectively. Unless noted otherwise, the final potential was set equal to the redox potential so that the relative equilibrium concentration at E_f of $B1_{red}$ is 0.5 and the ET rate constants (k_{ET}) for oxidation and reduction are identical. Then, the relaxation constant is given by

$$\tau = \frac{1}{2k_{ET}} \quad (2)$$

so that the ET rate constant can readily be determined from a semilogarithmical plot of the data according to eq 1 (Figure 3).

In the same way, time-resolved SERR spectra were measured and analyzed for Cyt-*c* adsorbed on C_3-, C_6-, C_{11}-, and C_{16}-coated Ag electrodes (Figure 3). Also for these chain lengths, no conformational species other than the native Cyt-*c* could be detected in the stationary and time-resolved SERR spectra. For each SAM-coating, the potential jumps were carried out from negative initial potentials E_i to the respective redox potential E^0 which decreases with increasing chain length.[16] This direction of the potential jumps was associated with a higher long-term stability of the SERR signals than potential jumps in the reverse direction with initial potentials of $\sim+0.1$ V. Such positive potentials close to the oxidation potential of Ag obviously cause the destruction of the SAMs and the decrease of SER-activity so that the error associated with the kinetic analysis is substantially higher. Nevertheless, for the C_6-coating, the ET kinetics were also determined for a potential jump from $E_i = +0.12$ V to E^0 leading to rate constants of 150 ± 35 and 100 ± 40 s^{-1} for H_2O and D_2O, respectively. Within the experimental accuracy, these values are the same as those for the

(20) Döpner, S.; Hildebrandt, P.; Mauk, A. G.; Lenk, H.; Stempfle, W. *Spectrochim. Acta* **1996**, *A 51*, 573.

(21) Parthasarathi, N.; Hansen, C.; Yamaguchi, S.; Spiro, T. G. *J. Am. Chem. Soc.* **1987**, *113*, 3865.

(22) Wackerbarth, H.; Murgida, D. H.; Oellerich, S.; Döpner, S.; Rivas, L.; Hildebrandt, P. *J. Mol. Struct.* **2000**, in press.

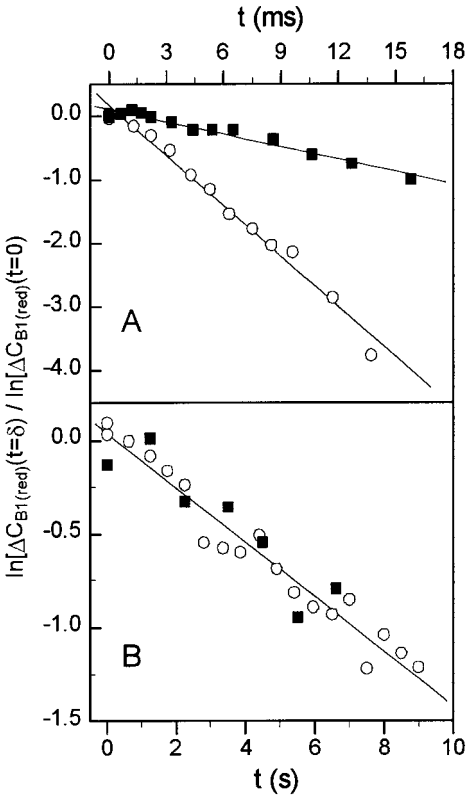

Figure 3. Semilogarithmic plots of the concentration changes of the reduced Cyt-*c* as a function of the delay time δ as determined by time-resolved SERR spectroscopy. $\Delta C(\delta)$ and $\Delta C(t_0)$ denote the deviations from equilibrium concentrations for E_f at $t = \delta$ and $t = 0$, respectively. (A) Cyt-*c* adsorbed on a C_2-coated Ag electrode with $E_i = -0.1$ V and $E_f = +0.0025$ V; (B) Cyt-*c* adsorbed on a C_{16}-coated Ag electrode with $E_i = -0.14$ V and $E_f = -0.039$ V. The solid squares and open circles refer to data obtained from experiments in H_2O and D_2O, respectively.

Table 1. Heterogeneous ET Rate Constants of Cyt-*c* on SAM-Coated Ag Electrodes

SAM	distance/ Å[a]	$k_{ET}(H_2O)$/ s^{-1}	$k_{ET}(D_2O)$/ s^{-1}	ratio $k_{ET}(H_2O)/k_{ET}(D_2O)$
C_2	6.3	132	33	4.0
C_3	7.6	128	64	2.0
C_6	11.5	134	109	1.2
C_{11}	19.0	43	42	1.0
C_{16}	24.0	0.073	0.074	1.0

[a] Distances refer to the length of ω-carboxylalkanethiols estimated as discussed previously.[16]

opposite jump from $E_i = -0.1$ V (134 ± 12 and 108 ± 6 s^{-1} for H_2O and D_2O, respectively).

The magnitude of the potential jump, that is, $|E_f - E_i|$, was adjusted to ≤ 0.1 V which was small enough to avoid interference with potential-dependent reorientational processes of the adsorbed Cyt-*c*.[17b] On the other hand, the potential jumps were associated with sufficiently large spectral changes as a prerequisite for a reliable spectra analysis. A complete list of the rate constants determined in this way is given in Table 1.

The results show a strong increase of the rate constant from the C_{16}-coated to the C_{11}-coated electrode by a factor of $\sim$600 followed by only a moderate increase for the C_6-coated electrode, whereas for the C_3- and C_2-SAMs essentially the same values were determined as for the C_6-SAM. This striking behavior is illustrated by a plot of the rate constants versus the length of the monolayers (Figure 4A).

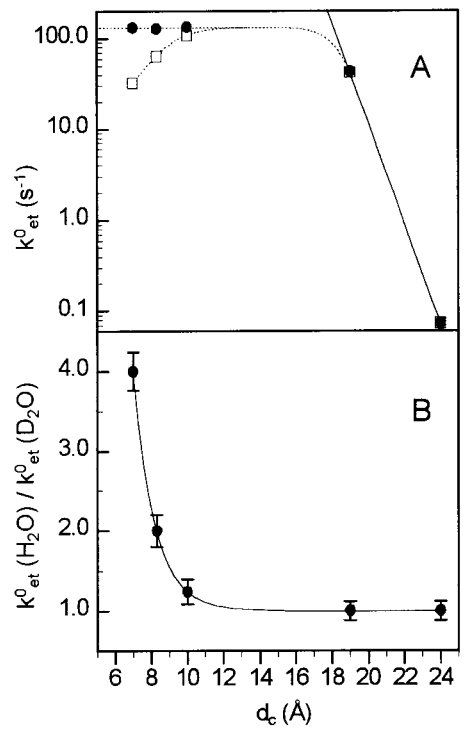

Figure 4. Distance dependence of the ET rate constants (A) and the kinetic H/D effect (B) as determined by time-resolved SERR spectroscopy as a function of the SAM-length (Table 1). The circles and squares in A refer to rate constants obtained from experiments in H_2O and D_2O, respectively.

Kinetic Isotope Effects. The time-resolved SERR experiments were also carried out in D_2O. Since H/D exchange has a negligible effect on the band frequencies of Cyt-*c* in the frequency range under consideration, the same component spectra could be used for the analysis of the SERR spectra. For C_{16}- and C_{11}-coated electrodes, time-resolved SERR experiments yielded ET rate constants that are identical to those obtained in H_2O. However, for shorter chain lengths, the rate constants in D_2O were found to be smaller than in H_2O and, furthermore, exhibit a maximum at the C_6-SAM (109 s^{-1}) and finally decays to a value as low as 33 s^{-1} at the C_2-SAM (Figure 4A, Table 1). This discrepancy in the distance dependence of the ET rate constants corresponds to a distance-dependent kinetic isotopic effect [$k_{ET}(H)/k_{ET}(D)$] that increases from 1.0 to 4.0 upon decreasing chain length (Figure 4B).

Experimental Accuracy and Errors. The kinetic analyses were based on three individual series of measurements for each potential jump. The semilogarithmical plots reveal a good linear correlation, and the overall error of the rate constants was estimated to be less than 10%. Thus, the deviations from the expected distance dependence of the ET rate constants are clearly beyond the error limits. We can also safely rule out that these deviations result from experimental artifacts. First, the time-resolution of the setup is $\sim$150 μs so that the determination of rate constants up to 1000 or 2000 s^{-1} is possible. In fact, preliminary experiments were carried out with higher driving forces, and the resultant faster ET processes could readily be analyzed. Second, possible imperfections of the monolayers that may exist for C_6-, C_3-, and C_2-coatings might cause a less clearly defined ET distance for the adsorbed Cyt-*c* but cannot account for a chain-length-independent rate constant in H_2O. Such imperfections do not include domains of bare Ag surface where Cyt-*c* could be directly adsorbed. As shown previously,[16] at SAM-coated Ag electrodes the upper limit of Cyt-*c* adsorbed

to the bare metal is less than 0.5%. Third, no possible experimental artifacts can account for the dramatic decrease of the rate constant in D_2O. Hence, the rate constants determined in this work reflect the unique ET dynamics of the adsorbed Cyt-*c* on the coated Ag electrode.

Discussion

The kinetic H/D isotope effect on the measured ET rate implies that the interfacial redox reaction is coupled with a process involving the transfer of proton(s). On the basis of the present results, the nature of the proton transfer (PT) process, that becomes rate-limiting at short distances, cannot be determined unambiguously. Most likely, it corresponds to the rearrangement of the hydrogen-bonding network in the interior of the protein. In fact, NMR spectroscopic investigations have demonstrated that there are distinct redox-linked differences in the hydrogen-bonding interactions.[23] These changes particularly involve those peptide segments that surround the heme pocket and include the axial ligands but are also detectable at a considerable distance remote from the heme iron. Thus, even a net "long-distance" PT cannot be excluded.

In any case, a coupling of ET and PT may be required to compensate for the charge change of the heme iron and, hence, should occur in each redox reaction of Cyt-*c* regardless of the kind of reaction partner. However, to our knowledge, a kinetic H/D effect has not been observed for homogeneous bimolecular ET reactions in solution or for photoinduced intramolecular ET reactions of Cyt-*c* or soluble redox proteins in general. Consequently, this behavior must be related to the specific reaction conditions for Cyt-*c* adsorbed at the electrode interface where charge-transfer processes occur under the influence of an electric field.

Electric-Field Effects on the Heterogeneous Electron Transfer at Electrodes. For the diabatic ET between the adsorbed Cyt-*c* and the electrode, the formal heterogeneous ET rate constant at zero overpotential can be approximated by

$$k_{ET} = \frac{2\pi(H_{RP})^2}{\hbar\sqrt{4\lambda RT}} \exp\left(-\frac{\lambda}{4RT}\right) \quad (3)$$

where H_{RP} is the electronic coupling parameter.[8e,24] The reorganization energy λ can be expressed as the sum of the reorganization energies of the redox center λ_i, the protein λ_p, and the solvent λ_s,[25] that is:

$$\lambda = \lambda_i + \lambda_p + \lambda_s \quad (4)$$

For long-range ET, the distance dependence of k_{ET} is largely due to the electronic coupling parameter, and one obtains an approximate expression

$$k_{ET} = A \exp(-d\beta) \quad (5)$$

where d is the SAM length, β, the electronic tunneling factor, and A, a constant.[24] Such an exponential function has been shown to be an adequate description of the distance dependence of long-range intra- and intermolecular ET.[5f]

At long chain lengths, that is, at C_{16}- and C_{11}-SAMs, no H/D effects on the redox process of Cyt-*c* are observed, implying that proton and deuteron transfer are faster than electron tunneling. Moreover, on the basis of eq 5, the rate constants for C_{16}- and C_{11}-SAMs yield $\beta = 1.28$ Å^{-1} which is close to that for ET through proteins and along alkyl chains.[5e,26,27] Since also the value for A (1.45×10^{12} s^{-1}) is in agreement with previous results for redox proteins,[5e,27] it is concluded that in the absence of a rate-limiting PT the heterogeneous ET displays a "normal" behavior of a long-distance electron tunneling.

For the C_6-SAM, the "normal" distance dependence of the ET (eq 5) predicts a rate constant of 6×10^5 s^{-1} which is much higher than the experimentally observed rate constant of 132 s^{-1}. Within the experimental accuracy, the measured rate constants in H_2O appear to remain largely constant upon further lowering the SAM length, whereas in D_2O the rate constant is found to decrease strongly. Since with decreasing distance to the electrode, the potential drop across the electrode/SAM interface increases,[16] this unusual kinetic behavior is attributed to the electric field experienced by the adsorbed Cyt-*c*.

In the simplest explanation the electric field may cause an increase of the activation energy for those PT steps that are required for adaptation of the protein structure to the change of the heme oxidation state. Raising the activation energy lowers the probability that the ET reaction occurs in the intersection region of the potential curves via *electron tunneling*. Thus, *nuclear tunneling* becomes more and more important, but the tunneling frequency decreases with the increase of the potential energy barrier. This effect is more pronounced for deuterons than for protons so that the increase of the kinetic isotopic effect with shorter SAM lengths can readily be understood. It is interesting to note that the limiting value for the $k_{ET}(H_2O)/k_{ET}(D_2O)$ ratio of 4.0 at C_2-SAM coated electrodes is similar to that found for the enzymatic reaction of serine proteases where proton/deuteron tunneling in a hydrogen-bonding network constitutes the rate-limiting step.[28,29]

Since the activation energy for the rearrangement of the hydrogen-bonding network is directly related to λ_p, the reorganization energy (eq 3 and 4) becomes a function of the electric field and, hence, increases with the (reciprocal) distance to the electrode. Note that in solution, that is, in the absence of an external electric field, the reorganization energy of the medium is expected to display the opposite distance dependence.[5e,24] Thus, even neglecting an electric field effect on the H_{RP},[30] the ET rate constant displays a rather complex dependence on the transfer distance.

Upon adsorption in the electrical double layer of the bare Ag electrode, the strength of the electric field experienced by the protein should be much higher than in the case of coated electrodes. In fact, for the native B1 state of the directly adsorbed Cyt-*c* as well as of the structurally related cytochrome c_{552} the ET rate constant was determined to be as low as ~4 s^{-1} even in H_2O.[14c,22]

An alternative model that may as well account for the observed kinetic behavior is based on a sequential reaction

(23) (a) Gao, Y.; Boyd, J.; Pielak, G. J.; Williams, R. J. P. *Biochemistry* **1991**, *30*, 1927. (b) Gao, Y.; McLendon, G.; Pielak, G. J.; Williams, R. J. P. *Eur. J. Biochem.* **1992**, *204*, 337.

(24) Marcus, R. A.; Sutin, N. *Biochim. Biophys. Acta* **1985**, *811*, 265.

(25) Basu, G.; Kitao, A.; Kuki, A.; Go, N. *J. Phys. Chem. B* **1998**, *102*, 2085.

(26) Finklea, H. A.; Hanshew, D. D. *J. Am. Chem. Soc.* **1992**, *114*, 3174.

(27) In proteins, β lies in the range between 1.1 and 1.4 Å^{-1} depending, inter alia, on the value chosen for the radius of the redox site.[5e] In eq 5, we have implicitly assumed that the protein surface represents the edge of the redox site. Literature data for the preexponential factor A refer to the maximum ET rate ($\Delta G = -\lambda$), which accounts for the higher values (~10^{13} s^{-1}) compared that determined in this work.

(28) Krishtalik, L. I. *Biochim. Biophys. Acta* **2000**, *1458*, 6.

(29) In the absence of hydrogen bonds, PT steps exhibit much larger kinetic isotopic effects.[28]

(30) The effect of the electric field on H_{RP} is likely to be smaller than that on the reorganization energy (Franzen, S.; Boxer, S. G. *Adv. Chem. Ser.* **1991**, *228*, 9. Nadtochenko, V. A.; Lavrentyev, A. I.; Rubtsov, I. V.; Denisov, N. N.; Barannikova, Y. V.; Nikandrov, V. V.; Krasnovsky, A. A. *Photochem. Photobiol.* **1991**, *53*, 261).

mechanism with the ET preceding or following the PT.[31] This model implies that there are two intermediate states, corresponding to local minima on the potential surface, in which the protein structure, that is, the hydrogen-bonding network, is not yet adapted to the respective oxidation states of the heme iron. In this case, the electric field may impose different potential energy barriers for each reaction step, that is, PT and ET. Whereas at low field strengths (i.e., at long distances), the ET step is slow compared to the PT steps, and the latter become rate-limiting with increasing field strength. Thus, in the course of the redox process, these intermediate states should be populated to an extent that exclusively depends on the respective ET and PT rate constants. Since SERR spectroscopy selectively probes the vibrational spectra of the heme group, this technique would only be capable of distinguishing between the intermediates and the stable forms if the changes of the hydrogen-bonding network are associated with conformational changes of the heme group. The time-resolved SERR spectra provide no indication for contributions from species other than the oxidized and reduced forms of the native B1 state of Cyt-*c*. If such intermediates are formed at all, they must have SERR spectra very similar to those of the respective stable oxidation states or their relative contributions must be very small during the relaxation processes.

Both models are compatible with the experimental results, and further studies are required to distinguish between the one-step and two-step reaction mechanism. On the other hand, the analysis of the SERR spectra also rules out the involvement of other non-Faradaic reactions in the overall redox process. First, there is no coupling with a conformational transition that involves a perturbation of the heme pocket and could affect the ET process, since such a structural change would be sensitively reflected by the SERR spectra. Specifically, the unique vibrational band pattern of the conformational state B2, which can be formed on bare electrodes and, under certain conditions, also on SAM-coated electrodes, allows an unambiguous distinction from the native B1 state.[16] However, in the present work, the B2 state does not contribute to the SERR spectra since the experiments were carried out with an excess of Cyt-*c* in the bulk solution which prevents the population of the B2 state for the adsorbed Cyt-*c*.[16,32] Consequently, the kinetic data extracted from the time-resolved SERR experiments exclusively refer to the native B1 state and any interference with the electric-field induced formation of B2 can be ruled out. Second, regardless of the SAM-length, the kinetics are monophasic, that is, they can be ascribed by a one-step relaxation process between the reduced and oxidized forms of the native state B1. Thus, a coupling with reorientational processes of the adsorbed Cyt-*c* can safely be excluded. Moreover, such reorientational processes occur on the long millisecond-time scale and are only induced by relatively large potential jumps,[17b] so that they cannot constitute the limiting step in the redox process of adsorbed Cyt-*c* at short SAM lengths as recently suggested by Avila et al.[8k]

Conversely, the results of the electroreflectance study of these authors can consistently be explained on the basis of an electric-field-dependent proton-coupled ET. For the ET kinetics of Cyt-*c* on SAM-coated Au electrodes, Avila et al.[8k] have observed a distance dependence of the heterogeneous ET constants that is qualitatively similar to our findings. However, the limiting value for the rate constant at short distances reported in that study is substantially higher ($\sim$1500 s^{-1}) than that determined in this work (130 s^{-1}). This discrepancy can be attributed to weaker electric fields at the Au/SAM interface and, hence, a higher limiting PT rate, compared to the Ag electrode. This conclusion is consistent with the fact that for C_{11}-coatings, for which even at Ag electrodes no electric field effect on the kinetics is observed [$k_{ET}(H_2O)/k_{ET}(D_2O) = 1.0$; Table 1], the rate constants are quite similar for the Au/SAM ($\sim$35 s^{-1})[8k] and Ag/SAM interface (43 s^{-1}; Table 1). Furthermore, the redox-linked reorganization of the hydrogen-bonding network also provides a reasonable explanation for the viscosity, ionic strength, and pH dependence of the ET kinetics observed by Avila et al.[8k]

Also the ET rate constants for Cyt-*c* on SAM-coated Au electrodes, which are obtained by cyclic voltammetry in Bowden's group,[8h] indicate a deviation from the "normal" distance dependence since for C_8- and C_{11}-coatings the respective rate constants of 1000 and 72 s^{-1} would correspond to an exponential decay factor of 0.6 $Å^{-1}$ that is lower by a factor of 2 compared to that for a "normal" intramolecular ET. For both distances, the rate constants are higher than those reported by Avila et al.,[8k] which may result from an intrinsic overestimation of ET rate constants in cyclic voltammetric experiments.[33]

Implications for Biological Electron-Transfer Reactions. In each redox reaction, the change of the charge at the redox center that is associated with an ET step must be compensated by the displacement of charged groups, ions, or protons in the immediate molecular environment. For redox centers that are embedded in a protein matrix and shielded against the solvent, charge compensation must primarily occur via the movement of amino acid side chains and the translocation of protons inside the protein. In electron-transferring proteins, unlike redox enzymes, these redox-linked structural changes are relatively small so that they can only be identified on the basis of well-resolved X-ray- and NMR-structures.[5e] Such data are available only for a few redox proteins such as Cyt-*c*,[3b,23] cytochrome c_2 from *Rhodobacter capsulatus*,[34] and cytochrome c_3 from various *Desulfovibrio* species.[35] For each of these proteins, redox-linked structural changes include alterations of the hydrogen-bonding network, which may even affect protein regions remote from the metal center. In essence, the reorganization of the hydrogen-bonding network could result in a directional proton translocation. Such a PT process may even be of further functional relevance within the concept of "energized protons" as recently discussed for cytochrome c_3.[35a,b]

Whereas for proteins in solution internal hydrogen-bond rearrangements are likely to be faster than long-range ET steps, sufficiently strong electric fields acting on immobilized proteins may affect the dynamics of the redox reactions such that the reorganization of the protein structure associated with the ET can be resolved kinetically. This generalization of the present findings for Cyt-*c* adsorbed on SAM-coated electrodes appears

(31) As another possible mechanism, in addition to a sequential ET/PT, Williams suggested a directly coupled electron/proton movement corresponding to a non-Franck−Condon process.[5e]

(32) In the absence of excess Cyt-*c* in solution, the portion of B2 formed on SAM-coated Ag electrodes increases with decreasing chain length, i.e., increasing electric field strength,[16] whereas on bare Ag electrodes, B2 is formed even in the presence of Cyt-*c* in solution.[11,12] Conformational changes of the heme pocket structure of Cyt-*c* that are associated with the redox process at an electrode have also been detected by Soret-CD and -MCD spectroscopy (Yuan, X.; Sun, S.; Hawkridge, F. M.; Chlebowski, J. F.; Taniguchi, I. *J. Am. Chem. Soc.* **1990**, *112*, 5380).

(33) Honeychurch, M. J. *Langmuir* **1998**, *14*, 6291.

(34) Zhao, D. Z.; Hutton, H. M.; Gooley, P. R.; MacKenzie, N. E.; Cusanovich, M. A. *Protein Sci.* **2000**, *9*, 1828.

(35) (a) Turner, D. L.; Salgueiro, C. A.; Catarino, T.; LeGall, J.; Xavier, A. V. *Eur. J. Biochem.* **1996**, *241*, 723. (b) Louro, R. O.; Catarino, T.; Turner, D. L.; Piçarra-Pereira, M. A.; Pacheco, I.; LeGall, J.; Xavier, A. V. *Biochemistry* **1998**, *37*, 15808. (c) Messias, A. C.; Kastrau, D. H.; Costa, H. S.; LeGall, J.; Turner, D. L.; Santos, H.; Xavier, A. *J. Mol. Biol.* **1998**, *281*, 719. (d) Brennan, L.; Turner, D. L.; Messias, A. C.; Teodoro, M. L.; LeGall, J.; Santos, H.; Xavier, A. V. *J. Mol. Biol.* **2000**, *298*, 61.

to be justified since there is no indication that these electric field effects are restricted to this specific protein or to the electrochemical device. This conclusion is of particular importance for redox proteins that are integrated in or bound to membranes and, hence, may experience electric fields generated by potential gradients across the membrane and local Coulombic interactions due to electrostatic binding. If these electric fields are of a strength comparable to those at electrodes, the redox reactions of such immobilized proteins may be affected in a qualitatively similar way so that dynamics and mechanism of their ET processes are not necessarily identical to those of the solubilized or dissolved proteins studied in vitro.

This has in fact been shown specifically for the redox reaction between Cyt-*c* and its natural membrane-bound reaction partner cytochrome *c* oxidase (CcO),[36] which prior to the interprotein ET, form an electrostatically stabilized complex.[1a] Using intact mitochondria and phospholipid vesicles reconstituted with CcO, it was found that the transmembrane potential gradient built up during the enzymatic process has a substantial effect on the intra- and intermolecular ET as well as on the proton translocation.[36] Specifically, it has been demonstrated that an increase of the transmembrane potential slows down and eventually blocks the interprotein ET. However, it is not yet clear whether the potential gradient affects the structure of the redox sites or the kinetics of the individual reaction steps or both.

The present and previous studies[16,17] on Cyt-*c* adsorbed on SAM-coated electrodes have demonstrated that two different processes can be induced by external electric fields. First, as shown in this work, the rate of protein reorganization or PT steps associated with the ET of Cyt-*c* may be reduced due to an increase of the activation energy or potential energy barrier, respectively. Second, the conformational transition from the native state of Cyt-*c*, B1, to the state B2 may be induced.[16] In the latter state, the redox potential is strongly shifted to negative values due to the change in the axial ligation pattern.[11,22] This transition is particularly favored for the oxidized state and may block the binding domain inasmuch as its binding constant is likely to be higher than that of the native oxidized Cyt-*c* (B1).[22] Each of these mechanisms or a combination of both can account for a slowing of the interprotein ET that occurs when the transmembrane potential is built up during the enzymatic turnover.[36]

Finally, electric fields may also affect the internal charge-transfer processes in CcO via perturbations of the redox site structures and modulations of the kinetics of individual ET or PT steps.

(36) (a) McGovern Moroney, P.; Scoles, T. A.; Hinkle, P. C. *Biochemistry* **1984**, *23*, 4991. (b) Gregory, L.; Ferguson-Miller, S. *Biochemistry* **1989**, *28*, 2655. (c) Sarti, P.; Antonini, G.; Malatesta, F.; Brunori, M. *Biochem. J.* **1992**, *284*, 123. (d) Nicholls, P.; Butko, P. *J. Bioenerg. Biomembr.* **1993**, *25*, 137.

Conclusions

1. At large separations from the electrode, the heterogeneous ET of Cyt-*c* adsorbed on SAM-coated electrodes exhibits an exponential distance dependence that is similar to that of intramolecular ET of redox proteins. Therefore, it is concluded that at SAM lengths up to ≥ 19 Å, electric fields at the adsorption site are too weak to influence the ET kinetics.

2. Upon decreasing the SAM length, the electric field strength increases and affects the ET rate such that it becomes nearly constant at SAM lengths between 12 and 6 Å.

3. The kinetic H/D effect of the observed rate constants at such short ET distances indicates that PT steps become rate-limiting. These PT processes may either be part of the structural reorganization of the protein associated with the ET or reflect the formation or decay of discrete intermediates kinetically coupled with the ET step.

4. The dynamics of the PT processes are slowed upon decreasing SAM length, implying that under the influence of the electric field the activation energy or potential energy barrier is raised.

5. The electric field effects on the heterogeneous ET reaction are not restricted to the electrodes but may also occur at biomembranes. Thus, transmembrane potentials may control interprotein ET reactions under physiological conditions.

Acknowledgment. We highly appreciate valuable discussions with Wolfgang Schmickler and Antonio Xavier on proton-coupled electron-transfer processes. We thank Birgit Deckers, Ulrich Paul, Horst Schaller, and Hartmut Ulbrich for technical support and assistance. The work was supported by the Volkswagen-Stiftung. D.H.M. acknowledges a fellowship from the Alexander-von-Humboldt Stiftung.

JA004165J